

Investigation on Structural, Relative Stable, and Electronic Properties of Binary Al_nLi_n ($n = 2 - 12$) Clusters through Density Functional Theory

Lei SHI^{1,2,3}, Zhiqiang ZHOU^{1,2,3}, Tao QU^{1,2,3*}, Dachun LIU^{1,2,3},
Xiumin CHEN^{1,2,3}, Baoqiang XU^{1,2,3}, Bin YANG^{1,2,3}, Yongnian DAI^{1,2,3}

¹National Engineering Laboratory of Vacuum Metallurgy, Kunming University of Science and Technology, Kunming 650093, People's Republic of China

²Key Laboratory of Vacuum Metallurgy for Non-ferrous Metal of Yunnan Province, Kunming 650093, People's Republic of China

³State Key Laboratory of Complex Nonferrous Metal Resources Clean Utilization in Yunnan Province, Kunming 650093, People's Republic of China

crossref <http://dx.doi.org/10.5755/j01.ms.26.2.23558>

Received 11 June 2019; accepted 19 November 2019

In the present research, the structural, the relative stable, and the electronic properties of Al_nLi_n ($n = 2 - 12$) clusters were investigated by density functional theory (DFT). By comparing the calculated values of Al_2 and Li_2 dimers with experimental ones, the reliability of the proposed method was proved. Furthermore, by considering the values of average binding energy (E_b), vertical ionization potential (VIP), vertical electron affinity (VEA), fragmentation energy (ΔE), second-order energy difference (Δ_2E), HOMO-LUMO (HL) gap, and chemical hardness (η) were calculated. It was found Fragmentation energy, second-order energy difference, VIP, VEA, the chemical stability and HOMO-LUMO gap exhibit odd-even oscillatory behaviours along with cluster size and have extreme values at $n = 5$ revealed Al_5Li_5 cluster yielded excellent stability. Those can be well explained by the density of states (DOS) that Li and Al atoms with stronger covalent bonds. Therefore, Al_5Li_5 cluster can be used as an ideal candidate for calculating Wilson parameters of Al-Li alloys.

Keywords: Al_nLi_n clusters, density functional theory, structural, relative stable, electronic properties.

1. INTRODUCTION

Due to its high plasticity, good electrical conductivity, good light reflectivity, strong corrosion resistance and extremely low magnetic permeability, high-purity aluminum is widely used in electronics, energy, transportation, computer, aerospace, astronomy and chemical industries [1–3]. Vacuum distillation as one of the green and efficient way of preparing high purity aluminum is received lots of attention from scholars [4–6]. In the previous work, we studied the vacuum purification experiment of aluminum. The experimental results indicate that Li is difficult to satisfactorily remove from Al. The vapour-liquid equilibrium (VLE) phase diagram has a significant advantage in guiding experiments and industrial production in vacuum distillation. However, clusters may reflect properties of the respective associated bulk alloy or the alloy melt to a certain extent.

The density functional theory is used to calculate the Al_nLi_n ($n = 2 - 12$) clusters, and the structural evolution of the Al-Li alloy system can be revealed from the atomic level to obtain a stable cluster structure. This will lay a solid theoretical foundation for the calculation of Wilson parameters of Al-Li alloy and the theoretical drawing of VLE phase diagram of Al-Li alloy, and finally provide theoretical guidance for the preparation of high-purity

aluminum by vacuum distillation. Therefore, obtaining Al_nLi_n clusters that can reflect the properties of Al-Li alloys is important.

A metal cluster generally consists of two or more atoms, molecules, and ions [7] and creates a bridge between microparticles and macroparticles [8], and small clusters demonstrate remarkable adsorption, optical, and catalytic properties [9]. It is already proved that small bimetallic clusters reveal nonmetallic properties, whereas large clusters exhibit metallic properties. Generally, metal clusters provide significant information on novel properties of nanomaterials at the atomic level. It is well known that size and shape are the main dominating factors that affect the physical and the chemical properties of metal clusters; therefore, it is imperative to investigate their structural and electronic properties as a function of cluster size (n). In recent years, researchers have employed the ab-initio molecular dynamics (AIMD) simulation method to measure different properties of metal clusters [10–12].

Cox et al. [13] observed the magnetic phenomenon in aluminum (Al_n) clusters and concluded that each Al_n ($n \leq 9$) cluster had a magnetic moment. Akola et al. [14] found that the growth of Al_n ($12 \leq n \leq 23$) clusters was governed by the addition and subtraction of atoms on the basis of the icosahedral structure of Al_{13} . Chuang et al. [15] noticed that the most stable structure of Al_{19} was formed after the

* Corresponding author. Tel.: +86-13518715200.

E-mail address: qutao_82@126.com (T. Qu)

addition of five adjacent atoms and monoatoms to the icosahedron. Rao et al. [16] analyzed the magnetic properties of Al_n ($1 \leq n \leq 15$) clusters and indicated that when $n \leq 10$, the average atomic magnetic moments of odd and even atoms were, respectively, $1 \mu B$ and $2 \mu B$; however, when $n \geq 10$, the magnetic moment of the cluster disappeared completely. Li et al. [17] observed that the most stable structure of Al_n clusters was changed from planar to stereostructure when $n = 6$, and the stability of Al_7 clusters was higher than that of adjacent clusters. The average magnetic moments of Al_n clusters were obtained as $2 \mu B$ when $n = 2, 4$, and 6 , and $1 \mu B$ when $n = 1, 3, 5, 7$, and 9 .

Lithium (Li) is the lightest element among metals and can be regarded as a model of near-free electron system; thus Li clusters are considered as the basis for discussing the electronic structures of heavy metal clusters. Boustani et al. [18] studied the relationship between electronic structures and symmetry of small Li clusters based on the ab-initio method. Gardet et al. [19] investigated the structural and the electronic properties of small Li_n clusters ($n = 20$) through density functional theory (DFT). Fournier et al. [20] revealed different properties of Li_n ($n = 5 - 20$) clusters based on the Kohn-Sham theory using local spin density and modified gradient energy functionals.

The small specific gravity of Li and the high solubility in Al are the main attributes of AlLi clusters. AlLi clusters have attracted considerable scientific attention due to their lightweights and high strengths. C. Majumder et al. [21] studied Al_nLi ($n = 1, 13$) clusters using ab initio density-based molecular dynamics, the results indicate that the Li atom segregates to the surface of the aluminum cluster and prefers to form a tetrahedron, wherever possible, with one of the triangular faces of Al atoms. In particular, for $Al_{13}Li$, the Al_{13} core takes the most symmetric icosahedral form with the Li atom occupying the outer ‘hollow-site’. Cheng et al. [22] investigated the electronic and the structural properties of small LiAl clusters based on a local spin density functional method in combination of a non-local pseudopotential. Akola et al. [23] examined the geometries and the electronic properties of small Li-rich Al_NLi_5N ($N = 1 - 6, 10$) clusters based on first-principle simulations and observed a significant charge transfer from Li atoms to nearby Al atoms (thus resulting in the strengthening of ionic bonds between Li and Al atoms) and the formation of Al-Al covalent bonds. Kumar [24] also observed such a charge transfer by in Al-Li clusters.

Based on the interaction energy parameters of clusters, Yang et al. [25] and Chen et al. [26] combined with Wilson equation to predict the activity and VLE phase diagram of binary Pb-Ag, Pb-Pd and Pb-Pt Alloys systems. The result

shows that the theoretically predicted activity and VLE phase diagram agree well with the experimentally measured.

In the current work, the structural, the relative stable, and the electronic properties of Al_nLi_n ($n = 2 - 12$) clusters were investigated by DFT.

2. COMPUTATIONAL METHODS

In the present work, DFT calculations [27, 28] were carried out on the DMol³ code [7]. The GGA-PBE functional was adopted to analyze exchange-correlation interactions, and the all-electron relativistic was considered to treat the core. The double numerical basis with polarized functions (DNP) was employed to formulate the basis set, and in order to achieve good convergence results, smearing with a value of 0.005 Ha was considered. Furthermore, for geometry optimization, the values of maximum displacement tolerance, energy tolerance, and maximum force tolerance were set to 0.005 \AA , 10^{-5} Ha/atom , and 0.002 Ha/\AA , respectively. During ab-initio molecular dynamics simulations, the temperature of the system was set to 300 K , and the total simulation time was set to 100 ps with a time step of 1 fs . Stable structures were further determined by frequency calculations, and in order to ensure the accuracy, parameters of Al_2 and Li_2 were calculated (Table 1).

3. RESULTS AND DISCUSSION

3.1. Ground structures of Al_nLi_n ($n = 2 - 12$) clusters

The initial structures of Al_nLi_n ($n = 2 - 12$) clusters were first optimized by geometry optimization, and the optimized structures were then used for ab-initio molecular dynamics (AIMD) calculations in order to obtain low-lying isomers of Al_nLi_n clusters. Low-lying isomers were further optimized to perform energy calculations, and finally, ground-state structures of Al_nLi_n clusters were achieved.

Fig.1 displays the ground structures of Al_nLi_n ($n = 2 - 12$) clusters. It is discernible that the shape of Al_2Li_2 was quadrilateral with the symmetry group of C_2 . When $n = 3$, a pyramid (with the symmetry group of C_1) was formed with three Al atoms and two Li atoms at the bottom, and one Li atom at the top. The Al_4Li_4 cluster (with the symmetry group of C_1) revealed the shape of a hat with one Al atom at the top, two Li atoms and two Al atoms at the middle, and two Li atoms and one Al atom at the bottom. The Al_5Li_5 cluster (with the symmetry group of C_1) also yielded the shape of a hat. The Al_6Li_6 cluster manifested a prolate structure with a symmetry group of C_1 .

Table 1. Calculated and experimental values of bond lengths (R), binding energies (E_b), frequencies (ω), and vertical ionization potentials (IP s) of Al_2 and Li_2

		$R, \text{ \AA}$	$E_b \text{ (eV)}$	$\omega, \text{ cm}^{-1}$	$IP, \text{ eV}$
Li ₂	Expt [19]	2.67	0.53	351	5.14
	GGA-PBE	2.633	0.5762087	368.58	5.10889
Al ₂	Expt [20]	2.701	1.34 ± 0.06	284.2	6.20
	Expt [20]	2.701 ± 0.002	1.36	286	
	GGA-PBE	2.679	1.44993	302.97	6.3838618

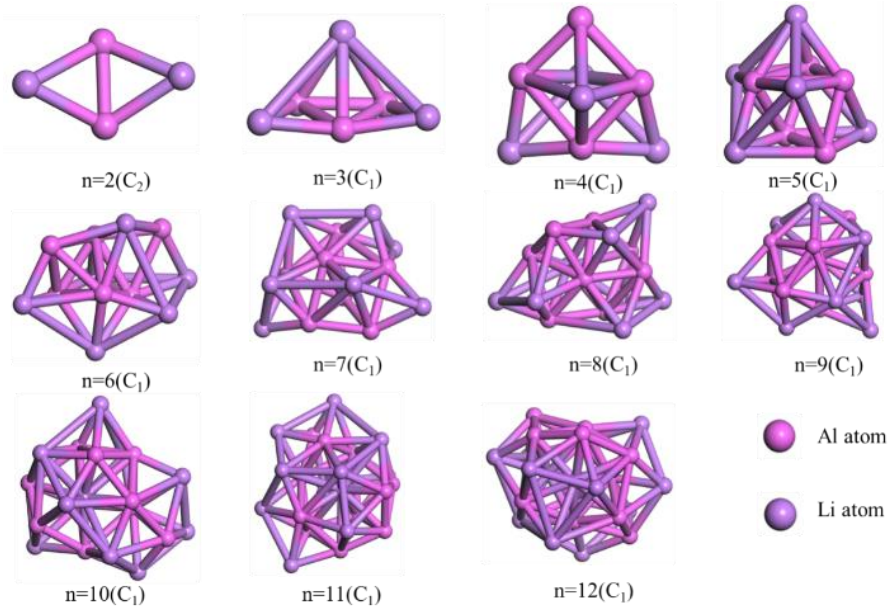


Fig. 1. Ground state structures of Al_nLi_n ($n = 2 - 12$) clusters

From $n = 7$ to 12, clusters were irregular and densely packed without any symmetry. Therefore, it can be inferred that the symmetry of Al_nLi_n clusters started to decrease with the increasing cluster size. Overall, there are a common tendency that Al atoms and Li atoms occupy the apex of the Al_nLi_n ($n = 2 - 12$) cluster structure, and Li atoms are not found to be surrounded by Al atoms, consistent with the results of studies [21].

3.2. Relative stable properties of Al_nLi_n ($n = 2 - 12$) clusters

Calculated values of $E(\text{Al}_n\text{Li}_n)$, $E(\text{Al})$, $E(\text{Li})$, $E(\text{Al}_n\text{Li}_n^+)$, $E(\text{Al}_n\text{Li}_n^-)$, HOMO and LUMO are shown in Table 2.

The binding energies (E_b) for the Al_nLi_n clusters are defined as:

$$E_b = [nE(\text{Al}) + nE(\text{Li}) - E(\text{Al}_n\text{Li}_n)] / 2n, \quad (1)$$

where $E(\text{Al})$, $E(\text{Li})$, and $E(\text{Al}_n\text{Li}_n)$ represent the energies of Al atoms, Li atoms, and Al_nLi_n clusters. The Binding energy is an important parameter that can denote the thermodynamic stabilities of clusters. As can be seen from Fig. 2, the E_b of Al_nLi_n ($n = 2 - 12$) clusters monotonically

rise as the cluster size evolves which indicates that the stability of Al_nLi_n ($n = 2 - 12$) clusters were enhanced with the increasing of cluster size. Furthermore, E_b increase dramatically with cluster size from $n = 2$ to $n = 5$, and then becomes smooth ($n = 5$ to $n = 12$). It is suggested that the Al_nLi_n ($n \geq 5$) clusters may reflect properties of the respective associated AlLi alloy to a certain extent.

Fragmentation energies (ΔE) for the Al_nLi_n clusters are defined as:

$$\Delta E(\text{Al}_n\text{Li}_n) = E(\text{Al}_{n-1}\text{Li}_{n-1}) + E(\text{AlLi}) - E(\text{Al}_n\text{Li}_n), \quad (2)$$

where $E(\text{Al}_n\text{Li}_n)$, $E(\text{Al}_{n-1}\text{Li}_{n-1})$, and $E(\text{AlLi})$ are energies of Al_nLi_n , $\text{Al}_{n-1}\text{Li}_{n-1}$, and AlLi clusters, respectively. Values for fragmentation energies reflect the energies required during the dissociation of Al_nLi_n into AlLi and $\text{Al}_{n-1}\text{Li}_{n-1}$ clusters, and it signifies that high fragmentation energy could result in a stable cluster. It can be seen from the Fig. 3 that odd-even alternation behavior as a function was exhibited of cluster sizes from $n = 4$ to 12. The local peaks are observed at $n = 5, 7, 9$ and 11, denoting that odd clusters have higher stability than their neighbors except for $n = 3$. Al_5Li_5 cluster has a higher fragmentation energy than other odd clusters.

Table 2. Calculated values of $E(\text{Al}_n\text{Li}_n)$, $E(\text{Al})$, $E(\text{Li})$, $E(\text{Al}_n\text{Li}_n^+)$, $E(\text{Al}_n\text{Li}_n^-)$, HOMO and LUMO

n	$E(\text{Al}_n\text{Li}_n)$, eV	$E(\text{Al})$, eV	$E(\text{Li})$, eV	$E(\text{Al}_n\text{Li}_n^+)$, eV	$E(\text{Al}_n\text{Li}_n^-)$, eV	HOMO, eV	LUMO, eV
1	-6795.699429						
2	-13594.44829	-6591.75387	-202.9509057	-13589.23172	-13595.03275	-2.92	-2.67
3	-20393.08188	-6591.75387	-202.9509057	-20388.04948	-20393.86398	-3.073	-2.632
4	-27192.41884	-6591.75387	-202.9509057	-27187.55856	-27193.25635	-2.96	-2.595
5	-33992.77974	-6591.75387	-202.9509057	-33987.73238	-33993.2778	-3.385	-2.024
6	-40791.23166	-6591.75387	-202.9509057	-40786.60307	-40792.20164	-3.163	-2.446
7	-47590.65323	-6591.75387	-202.9509057	-47586.18861	-47591.49147	-3.035	-2.215
8	-54389.5301	-6591.75387	-202.9509057	-54385.20007	-54390.59466	-2.889	-2.487
9	-61189.70334	-6591.75387	-202.9509057	-61185.32847	-61190.89705	-2.886	-2.638
10	-67988.08473	-6591.75387	-202.9509057	-67983.74643	-67989.36963	-2.956	-2.703
11	-74787.87834	-6591.75387	-202.9509057	-74783.56396	-74789.22884	-3.003	-2.723
12	-81587.19609	-6591.75387	-202.9509057	-81582.7997	-81588.66141	-3.111	-2.787

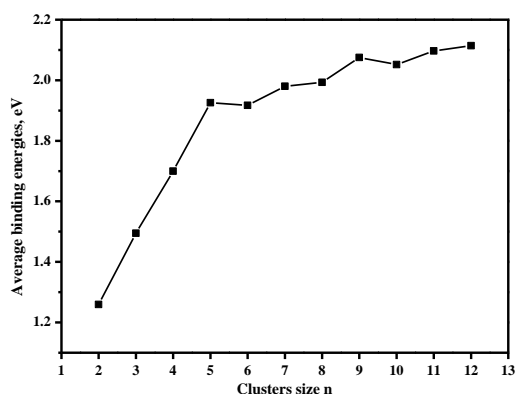


Fig. 2. Average binding energies of Al_nLi_n ($n = 2 - 12$) clusters

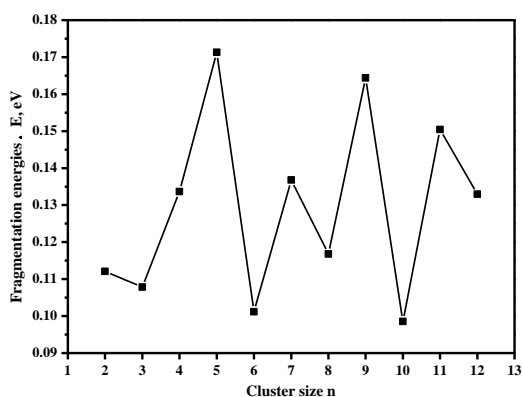


Fig. 3. Fragmentation energies of Al_nLi_n ($n = 2 - 12$) clusters

The second-order energies difference (Δ_2E) are defined as:

$$\Delta_2E(Al_nLi_n) = E(Al_{n-1}Li_{n-1}) + E(Al_{n+1}Li_{n+1}) - 2E(Al_nLi_n), \quad (3)$$

where $E(Al_{n+1}Li_{n+1})$, $E(Al_nLi_n)$, $E(Al_{n-1}Li_{n-1})$ are the energies of $Al_{n+1}Li_{n+1}$, Al_nLi_n , and $Al_{n-1}Li_{n-1}$ clusters, respectively.

The Second-order energies difference (Δ_2E) reflects the relative stability of the clusters between neighbors. From the Fig. 4 above we can see that the relationship between second-order energy difference and cluster size is presented.

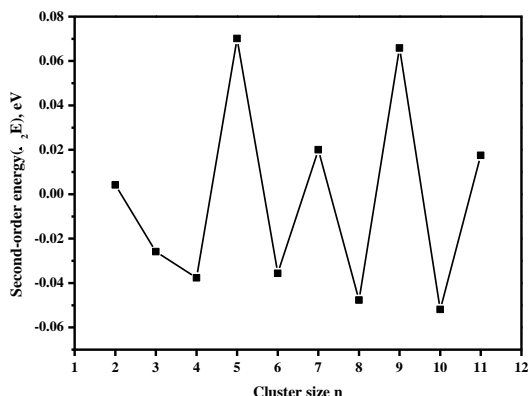


Fig. 4. Second-order energy differences of Al_nLi_n ($n = 2 - 12$) clusters

It can be observed that odd clusters have a higher second energy difference compared with even clusters. Clusters show an odd-even alternation of $n = 3 - 11$, except

for $n = 2$. The Al_5Li_5 , Al_7Li_7 , Al_9Li_9 , and $Al_{11}Li_{11}$ clusters, due to their higher values, manifested better stabilities as compared to their neighboring clusters.

3.3. Electronic properties of Al_nLi_n ($n = 2 - 12$) clusters

The vertical electron affinity (VEA) calculations and the vertical ionization potential (VIP) are parameters used for the characterization of the stability of a cluster.

The vertical electron affinity (VEA) reflects the binding energy of one neutral cluster that obtains one electron.

VEA is defined as:

$$VEA = E(Al_nLi_n) - E(Al_nLi_n^-), \quad (4)$$

where $E(Al_nLi_n)$ and $E(Al_nLi_n^-)$ are the energies of Al_nLi_n and $Al_nLi_n^-$ clusters.

Fig. 5. Shows the increase of VEA as the cluster size ($n = 2 - 12$) of Al_nLi_n evolves, except for $n = 3$ and 8. When n is between 3 and 8, an obvious odd-even pattern that VEAs of clusters with odd are lower than even. This means odd clusters are more stable than even and VEA has a minimum at $n = 5$.

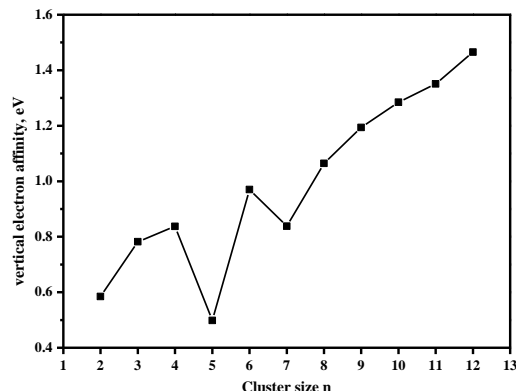


Fig. 5. The vertical electron affinity (VEA) of Al_nLi_n ($n = 2 - 12$) clusters

The vertical ionization potential (VIP) is a parameter commonly used to determine the stability of clusters. This is related to the bond energy of one cluster in neutral state that loses one electron.

VIP is defined as:

$$VIP = E(Al_nLi_n^+) - E(Al_nLi_n), \quad (5)$$

where $E(Al_nLi_n)$ and $E(Al_nLi_n^+)$ are the energies of Al_nLi_n and $Al_nLi_n^+$ clusters.

Values of VIP for Al_nLi_n ($n = 2 - 12$) clusters are presented in Fig. 6. It is observable that VIPs of Al_nLi_n clusters decreased significantly when the values of n ranged from 2 to 4 and 5 to 8; however, for $n = 9 - 12$, the values of VIP became stable. It is important to point out that the VIPs of Al_nLi_n increased sharply from $n = 4$ to 5. However, VIPs generally decreased significantly with the increasing cluster size, and it implies that neutral clusters easily lose one electron and become positive ones.

Chemical hardness is one of the global descriptors that measures the resistance of the molecular system to the deformation of its electron cloud or the resistance of the

system to charge transference [31].

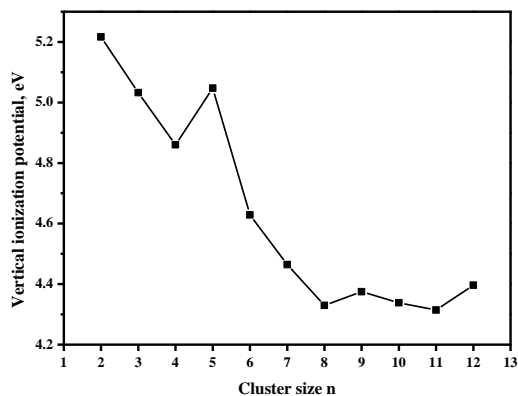


Fig. 6. VIPs of Al_nLi_n ($n = 2 - 12$) clusters

Chemical hardness (η) describes the chemical stability of a metal cluster. η is defined as:

$$\eta = \frac{VIP - VEA}{2}, \quad (6)$$

where VIP and VEA signify the vertical ionization potentials and vertical electron affinities, respectively.

The values of chemical hardness of Al_nLi_n clusters are depicted in Fig. 7. The local maximum values of chemical hardness were noticed at $n = 5$; hence, it expresses that Al₅Li₅ was more stable than their neighbouring clusters. Moreover, the chemical hardness (or stability) of Al_nLi_n clusters decreased significantly with the increasing cluster size.

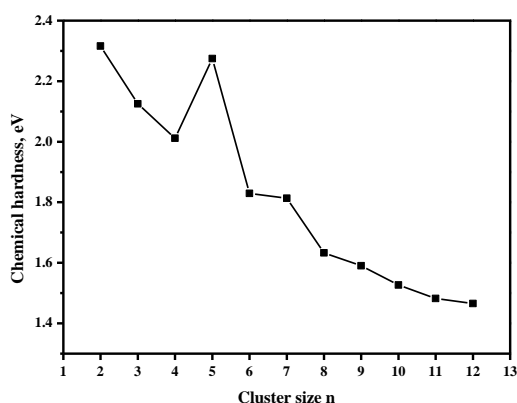


Fig. 7. Chemical hardness of Al_nLi_n ($n = 2 - 12$) clusters

The highest occupied-lowest unoccupied molecular orbital (HOMO-LUMO) energy gap is considered as a useful index to predict the stability of clusters. HOMO-LUMO (HL) gap is defined as:

$$HLgap = E_{HOMO}(Al_nLi_n) - E_{LUMO}(Al_nLi_n), \quad (7)$$

where $E_{HOMO}(Al_nLi_n)$ and $E_{LUMO}(Al_nLi_n)$ are the energy levels of HOMO and LUMO, respectively.

According to the frontier molecular orbital theory, the kinetic stability, the chemical stability, and the electrical conductivity of a metal cluster can be described by the energy gap between the highest occupied molecular orbital (HOMO) and the lowest unoccupied molecular orbital (LUMO). Generally, a high-energy HL gap makes a metal cluster more stable. Fig. 8 represents HL gaps of Al_nLi_n clusters. It is detectable that the HL gaps for odd Al_nLi_n

clusters were relatively higher and had a maximum at $n=5$, it reveals that Al₅Li₅ was more chemically stable than its adjacent clusters, and these results are well consistent with the findings of VIP, VEA, η , ΔE , and $\Delta_2 E$. Generally, the values of HL gap started to decrease with the increasing cluster size; thus Al_nLi_n manifested a trend of covalent-to-metallic transition, which is often observed in Al_n clusters [14].

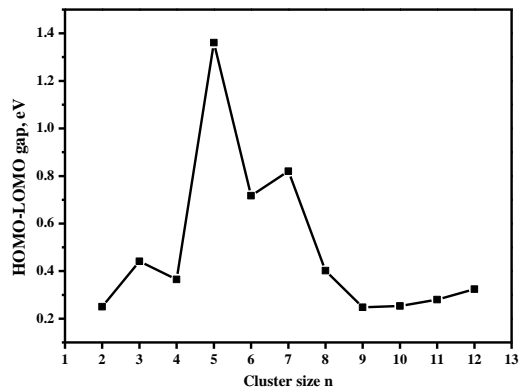


Fig. 8. HOMO-LUMO gaps of Al_nLi_n ($n = 2 - 12$) cluster

The density of states (DOS) of Al_nLi_n ($n = 2 - 12$) clusters were plotted in Fig. 9. It is evident that the DOS curves of Al_nLi_n clusters were mainly contributed by s and p electrons. The electronic states at the vicinity of Fermi level are mainly come from p states and the contribution of s is small. The continuities of DOS gradually became better, whereas the DOS curves had a negative shift (with the increasing cluster size) near the Fermi level. Therefore, with the increasing cluster size, overall energies of Al_nLi_n clusters become lower and the stability stronger. In the DOS, there are two spikes on both sides of the Fermi level, and the DOS between the two peaks is not zero, which is called "Pseudogap" [32]. The gap reflects the covalency of the bonding of the system: the wider Pseudogap, the stronger the covalency, the more stable of Al_nLi_n cluster. As we can see from Fig. 9, when $n = 5$, the enthalpy gap has the maximum value, indicating that the covalent bond of Al atom and Li atom is the strongest in Al₅Li₅ cluster, and the most stable of Al₅Li₅ cluster.

4. CONCLUSIONS

In the present paper, the structural, the relative stable, and the electronic properties of Al_nLi_n ($n = 2 - 12$) clusters were investigated by DFT calculations.

1. With the ground state structures of Al_nLi_n ($n = 2 - 12$) clusters, symmetry of Al_nLi_n clusters started to decrease with the increasing cluster size. Al atoms and Li atoms occupy the apex of the Al_nLi_n ($n = 2 - 12$) cluster structure, and Li atoms are not found to be surrounded by Al atoms, consistent with the results of studies.
2. Moreover, average binding energies of Al_nLi_n increased significantly with increasing cluster size. Fragmentation energy, second-order energy difference, VIP, VEA, the chemical stability and HOMO-LUMO gap exhibit odd-even oscillatory behaviours along with cluster size and have extreme values at $n = 5$ revealed that Al₅Li₅ had better stability as compared to their neighboring clusters.

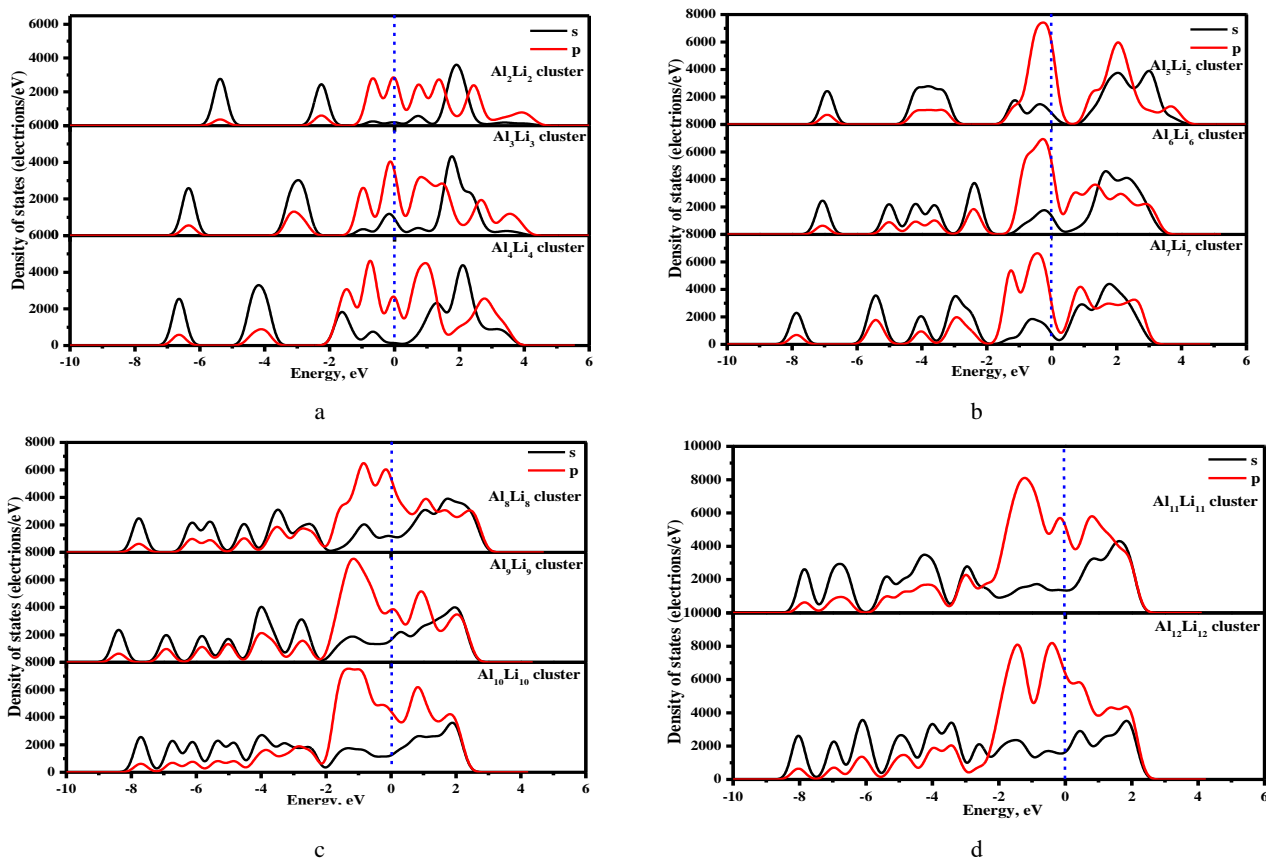


Fig. 9. Density of states of Al_nLi_n ($n = 2 - 12$) cluster: a – DOS for Al_nLi_n ($n = 2 - 4$) cluster; b – DOS for Al_nLi_n ($n = 5 - 7$) cluster; c – DOS for Al_nLi_n ($n = 8 - 10$) cluster; d – DOS for Al_nLi_n ($n = 11 - 12$) cluster

3. When cluster size $n = 5$, the enthalpy gap has the maximum value, indicating that the covalent bond of Al atom and Li atom is the strongest in Al_5Li_5 cluster, and the most stable of Al_5Li_5 cluster. Al_5Li_5 cluster can be used as an ideal candidate for calculating Wilson parameters of AlLi alloys.

Acknowledgment

The present project was financially supported by the National Natural Science Foundation, China (Grant No. 51604133) and the Academician Free Exploration Fund of Yunnan Province, China (Grant No. 2018HA006).

REFERENCES

- Kondo, M., Maeda, H., Mizuguchi, M. The production of high-purity aluminum in Japan *Jom* 42 (11) 1990: pp. 36 – 37.
<https://doi.org/10.1007/BF03220434>
- Shabestari, S.G., Gruzleski, J.E. Gravity segregation of complex intermetallic compounds in liquid aluminum-silicon alloys *Metallurgical and Materials Transactions A* 26 (4) 1995: pp. 999 – 1006.
<https://doi.org/10.1007/BF02649097>
- Matsubara, H., Izawa, N., Nakanishi, M. Macroscopic segregation in Al-11 mass% Si alloy containing 2 mass% Fe solidified under centrifugal force *Journal-Japan Institute of Light Metals* 48 (2) 1998: pp. 93 – 97.
- Belk, J. A. Vacuum techniques in metallurgy (Vol. 1), Pergamon Press. 1963: pp. 128 – 131.
- Winkler, O., Bakish, R. Vacuum Metallurgy. Elsevier, Amsterdam. 1971: pp. 161 – 162.
- Dai, Y.N. Vacuum Metallurgy of Nonferrous Metals. Metallurgical Industry Press, Beijing. 2009: pp. 34 – 50.
- Li, G.F., Wang, J.J., Chen, X.M., Yang, H.W., Yang, B., Xu, B.Q., Liu, D.C. Density functional investigation on structural and electronic properties of small bimetallic PbnAgn ($n = 2 - 12$) clusters *Journal of Central South University* 25 (0) 2018: pp. 772 – 782.
<https://doi.org/10.1007/s11771-018-3782-z>
- Zeng, Q., Shi, J., Jiang, G., Yang, M., Wang, F., Chen, J. Structures and optical absorptions of PbSe clusters from ab initio calculations *The Journal of Chemical Physics* 139 (9) 2013: pp. 094305 – 094305.
<https://doi.org/10.1063/1.481969>
- Li, G., Wang, J., Chen, X., Zhou, Z., Liu, D. Bimetallic PbnCun ($n=2-14$) Clusters Were Investigated by Density Functional Theory *Computational and Theoretical Chemistry* 1106 (0) 2017: pp. 21 – 27.
<https://doi.org/10.1016/j.comptc.2017.03.002>
- Issendorff, B.V., Cheshnovsky, O. Metal to insulator transitions in clusters *Annual Review of Physical Chemistry*. 56 (0) 2005: pp. 549 – 580.
<https://doi.org/10.1146/annurev.physchem.54.011002.103845>
- Wang, B., Zhao, J., Chen, X., Shi, D., Wang, G. Atomic structures and covalent-to-metallic transition of lead clusters Pb_n ($n = 2 - 22$) *Physical Review A* 71 (3) 2005: pp. 033201 – 033201.
<https://doi.org/10.1103/PhysRevA.71.033201>
- Heinzelmann, J., Kruppa, P., Proch, S., Kim, Y.D.,

- Ganteför, G.** Electronic relaxation in lead clusters: An indicator of non-metallic behavior *Chemical Physics Letters* 603 (0) 2014: pp. 1–6.
<https://doi.org/10.1016/j.cplett.2014.04.034>
13. **Cox, D. M., Trevor, D.J., Whetten, R.L., Rohlfing, E.A., Kaldor, A.** Aluminum clusters: Magnetic properties *The Journal of Chemical Physics* 84 (8) 1986: pp. 4651–4656.
<https://doi.org/10.1063/1.449991>
 14. **Akola, J., Häkkinen, H., Manninen, M.** Ionization potential of aluminum clusters *Physical Review B* 58 (7) 1998: pp. 3601–3601.
<https://doi.org/10.1103/PhysRevB.58.3601>
 15. **Chuang, F.C., Wang, C.Z., Ho, K.H.** Erratum: Structure of neutral aluminum clusters Al_n ($2 \leq n \leq 23$): Genetic algorithm tight-binding calculations *Physical Review B* 77 (7) 2008: pp. 125431–125431.
<https://doi.org/10.1103/PhysRevB.77.079904>
 16. **Rao, B.K., Jena, P.** Evolution of the electronic structure and properties of neutral and charged aluminum clusters: A comprehensive analysis *The Journal of Chemical Physics* 111 (5) 1999: pp. 1890–1904.
<https://doi.org/10.1063/1.479458>
 17. **Li, D.M., Wen, J.Q., Chen, H.X.** Density-functional theory study of the structures and properties of Al_n ($n = 2 - 10$) clusters *Journal of Northwest Normal University(Natural Science)* 54 (5) 2018: pp. 50–55.
<https://CNKI:SUN:XBSF.0.2018-05-010>
 18. **Boustani, I., Pewestorf, W., Fantucci, P., Bonaić-Koutecký, V., Koutecký, J.** Systematic ab initio configuration-interaction study of alkali-metal clusters: Relation between electronic structure and geometry of small Li clusters *Physical Review B* 35 (18) 1987: pp. 9437–9437.
<https://doi.org/10.1103/PhysRevB.35.9437>
 19. **Gardet, G., Rogemond, F., Chermette, H.** Density functional theory study of some structural and energetic properties of small lithium clusters *The Journal of Chemical Physics* 105 (22) 1996: pp. 9933–9947.
<https://doi.org/10.1063/1.472826>
 20. **Fournier, R., Bo Yi Cheng, J., Wong, A.** Theoretical study of the structure of lithium clusters *The Journal of Chemical Physics* 119 (18) 2003: pp. 9444–9454.
<https://doi.org/10.1063/1.1615237>
 21. **Majumder, C., Das, G.P., Kulshrestha, S.K., Shah, V., Kanhere, D.G.** Ground state geometries and energetics of Al_nLi ($n = 1, 13$) clusters using ab initio density-based molecular dynamics *Chemical Physics Letters* 261 (4–5) 1996: pp. 515–520.
[https://doi.org/10.1016/0009-2614\(96\)01028-7](https://doi.org/10.1016/0009-2614(96)01028-7)
 22. **Cheng, H.P., Barnett, R.N., Landman, U.** Energetics and structures of aluminum-lithium clusters *Physical Review B* 48 (3) 1993: pp. 1820–1820.
<https://doi.org/10.1103/PhysRevB.48.1820>
 23. **Akola, J., Manninen, M.** Aluminum-lithium clusters: First-principles simulation of geometries and electronic properties *Physical Review B* 65 (24) 2002: pp. 245424–245424.
<https://doi.org/10.1103/PhysRevB.65.245424>
 24. **Kumar, V.** Al 10 Li 8: A magic compound cluster *Physical Review B* 60 (4) 1999: pp. 2916–2916.
<https://doi.org/10.1103/PhysRevB.60.2916>
 25. **Yang, X., Chen, X., Zhang, C., Xie, X., Yang, B., Xu, B., Yang, H.** Prediction of vapor–liquid equilibria for the Pb-X ($X = Ag, Cu$ and Sn) systems in vacuum distillation using ab initio methods and Wilson equation *Fluid Phase Equilibria* 417 2016: pp. 25–28.
<https://doi.org/10.1016/j.fluid.2016.02.024>
 26. **Chen, X., Xu, B., Yang, B., Liu, D., Yang, H.** Prediction of Vapor–Liquid Equilibria for Pb–Pd and Pb–Pt Alloys Using Ab Initio Methods in Vacuum Distillation *Journal of Solution Chemistry* 46 (7) 2017: pp. 1514–1521.
<https://doi.org/10.1007/s10953-017-0658-z>
 27. **Deng, J., Lei, Y., Wen, S., Chen, Z.** Modeling interactions between ethyl xanthate and Cu/Fe ions using DFT/B3LYP approach *International Journal of Mineral Processing* 140 (0) 2015: pp. 43–49.
<https://doi.org/10.1016/j.minpro.2015.04.026>
 28. **Li, G.F., Zhou, Z.Q., Chen, X.M., Wang, J.J., Yang, H.W., Yang, B., Liu, D.C.** Structural, Relative Stable, and Electronic Properties of Pb_nSn_n ($n = 2 - 12$) Clusters were Investigated Using Density Functional Theory *Journal of Cluster Science* 28 (5) 2017: pp. 2503–2516.
<https://doi.org/10.1007/s10876-017-1242-9>
 29. **Venkataramanan, N.S., Suvitha, A., Note, R., Kawazoe, Y.** Structures of small Y_nAl_m clusters ($n + m \leq 6$): A DFT study *Journal of Molecular Structure: THEOCHEM* 902 (1–3) 2009: pp. 72–78.
<https://doi.org/10.1016/j.theochem.2009.02.017>
 30. **Fu, Z., Lemire, G.W., Bishea, G.A., Morse, M.D.** Spectroscopy and electronic structure of jet-cooled Al_2 *The Journal of Chemical Physics* 93 (12) 1990: pp. 8420–8441.
<https://doi.org/10.1063/1.459280>
 31. **Pearson, R.G., Pearson, R.G.** Chemical hardness and density functional theory *Journal of Chemical Sciences* 117 (05) 2005: pp. 11–25.
<https://doi.org/10.1007/BF02708340>
 32. **Song, B.Y.** Molecular Dynamics Simulation and Vacuum Distillation Experimental Study of Pb-Sb Alloy, Kunming University of Technology Press, Kunming. 2016: pp. 60–86.